Radiation effects in Si–Ge quantum size structures (review)

© N.A. Sobolev¶

Departamento de Física & I3N, Universidade de Aveiro,
3810-193 Aveiro, Portugal

(Получена 17 июля 2012 г. Принята к печати 20 июля 2012 г.)

The article is dedicated to the review and analysis of the effects and processes occurring in Si–Ge quantum size semiconductor structures upon particle irradiation including ion implantation. Comparisons to bulk materials are drawn. The reasons of the enhanced radiation hardness of superlattices and quantum dots are elucidated. Some technological applications of the radiation treatment are reviewed.

1. Introduction

The tolerance of materials and devices to radiation-induced defects (radiation defects, RDs) is of crucial importance in atomic energy and space applications. In a nuclear reactor, the samples are exposed to neutrons and gamma-quanta. The space-radiation environment accompanying most useful orbits consists of energetic electrons (energies up to ~ 7 MeV), protons (energies extending to hundreds of MeV) and small amounts of low energy heavy ions [1]. The LEO proton spectrum is especially hard: between 50 and 500 MeV the proton flux decreases only by a factor of 4.

Furthermore, the creation of RDs is an inevitable collateral effect in the ion implantation and neutron transmutation doping, as well as in particle detector applications. Finally, there is a possibility of using RDs themselves in the device technology. With the onrushing advent of quantum-size semiconductor structures (QSSS), the studies of RDs in them rapidly grow in importance.

The result of irradiating a semiconductor material will depend on the type of radiation, its mode (pulsed, continuous) and type of interaction with the material, as well as the type and temperature of the material. The two main types of interaction of radiation with materials are atomic displacements and ionization. All particles (electrons, protons, heavy ions and photons ranging from UV to gamma energies) except neutrons produce ionization effects in materials. Besides, the radiation effects in solid-state devices include single-event upsets.

When an energetic ion penetrates into a material, it loses energy mainly by two nearly independent processes: (i) elastic collisions with the nuclei known as nuclear energy loss, which dominates at an energy of about 1 keV/amu; (ii) inelastic collisions of the highly charged projectile ion with the atomic electrons of the matter known as electronic energy loss, which dominates at an energy of ~ 1 MeV/amu or higher. In the inelastic collision (cross-section $\sim 10^{-16}$ cm^2) the energy is transferred from the projectile ion to the atoms through excitation and ionization of the surrounding electrons. The amount of electronic loss in each collision varies from tens of eV to a few keV per Å [2].

¶ E-mail: sobolev@ua.pt

The atomic displacements occur due to the transfer of momentum of the incident particle to the atoms of the target material (nuclear energy loss). Provided an atom subjected to such a collision receives sufficient kinetic energy, it will be removed from its position and leave behind a vacancy. The removed atom may meet another such vacancy and recombine or lodge in an interstitial position in the lattice (a self-interstitial) or be trapped by an impurity atom. The vacancies may be mobile, too, and either combine with impurity atoms or/and cluster with other vacancies. Defects that are stable at the irradiation temperature may become mobile upon subsequent heating. For the evaluation of the radiation damage in solids the mobility of the defects is of paramount importance. The self-interstitials in silicon are mobile even at 0.5 K [3]. In Si and Ge a large part of the primary defects undergo annihilation even below room temperature (RT). The RDs in these materials, which are found at RT, consist mainly of secondary and tertiary complexes formed by migration and agglomeration of vacancies and interstitials with each other and with impurities. The resulting complexes are usually electronically active.

When the energy of the primary recoil atom is high, what is especially the case upon ion implantation or neutron irradiation, a collision cascade develops, where the defect density is much higher than upon electron or proton irradiation. This high defect density may lead to an amorphization of the implanted layer. The accompanying defect rearrangement processes are usually quite complex and not yet understood in all details even in elemental semiconductors such as Si and Ge.

The total cross-section for the displacement of an atom from its regular lattice site as a result of an elastic collision is given by [4]

$$\sigma(E) = \int_{T_d}^{T_m} d\sigma(E, T), \qquad (1)$$

where E is the kinetic energy of the incident particle, T is the kinetic energy transmitted to the lattice atom, $d\sigma(E, T)$ is the differential cross section of the corresponding interaction. The integration is performed over the energy T from the minimum energy T_d necessary for the displacement of a lattice atom into an interstitial position to the maximum energy T_m which the incident particle

can transmit to the target atom. The energy T_d is called threshold energy. The differential cross section depends on the interaction potential. In the case of charged particles (electrons, protons, ions) the interaction can be described by the Coulomb potential; for the neutral particles (neutrons) it is rather similar to the collision of hard spheres. The experimental values of T_d for silicon and germanium are equal to 21 eV and 27.5 eV, respectively [4]. To calculate the number of displacements produced by an incident particle, one has to solve the integral in Eq. (1), taking into account the type of interaction.

Collisions with neutrons are much harder in terms of the average energy transmitted to a target atom than those with protons of equal energy. The energy of electrons must achieve hundreds of keV in order to implement transfer of an energy amount exceeding T_d. On the contrary, in the case of the ions, the masses of the incident particle and the target atom are comparable, so that the energy transfer is very efficient, and even in the case of the ion etching of the surface with energies of hundreds of eV the creation of RDs must be taken into account. Fast neutron irradiation produces energetic recoil atoms and in terms of the produced damage can be understood as „internal" self-ion implantation. However, due to the small collision cross-section, the displacement cascades are well separated in the crystal volume even at moderate irradiation doses.

On the contrary, implantation of medium and heavy mass ions produces a very dense damage within a thin subsurface layer of a solid target, so that amorphization of this layer can be readily achieved. The critical fluence needed for the amorphization of a given crystal depends on the ion mass and the target temperature. For each ion–target combination, there is a critical temperature above which the amorphization becomes impossible due to dynamical defect annealing [5,6]. (At cryogenic temperatures, the amorphization of silicon was induced even under MeV electron irradiation, but the required fluences were exceedingly high [7,8].) The energy dependence of the critical ion fluence exists but is less pronounced. The theoretical description of the crystalline-to-amorphous transition upon ion irradiation is still a matter of debate [9]. Another important peculiarity of the ion irradiation is the sputtering of the target [10].

In practical terms, the SRIM/TRIM Monte Carlo simulation code [11] can be applied to calculate the ranges and primary displacement defects created by energetic ions in matter. To apply SRIM/TRIM to the calculation of the effects of other types of radiation, one additionally needs the „Integrated TIGER Series" (ITS code) for electrons and photons, or the „Monte Carlo Neutron Program" (MCNP code) for neutrons [12]. Electron trajectories and energy loss profiles can also be simulated using the CASINO code [13]. A few examples of the primary damage and implanted ion concentration profiles calculated by TRIM are given in Fig. 1.

It is important to note that the proton-induced damage profile is highly non-uniform with a sharp maximum near

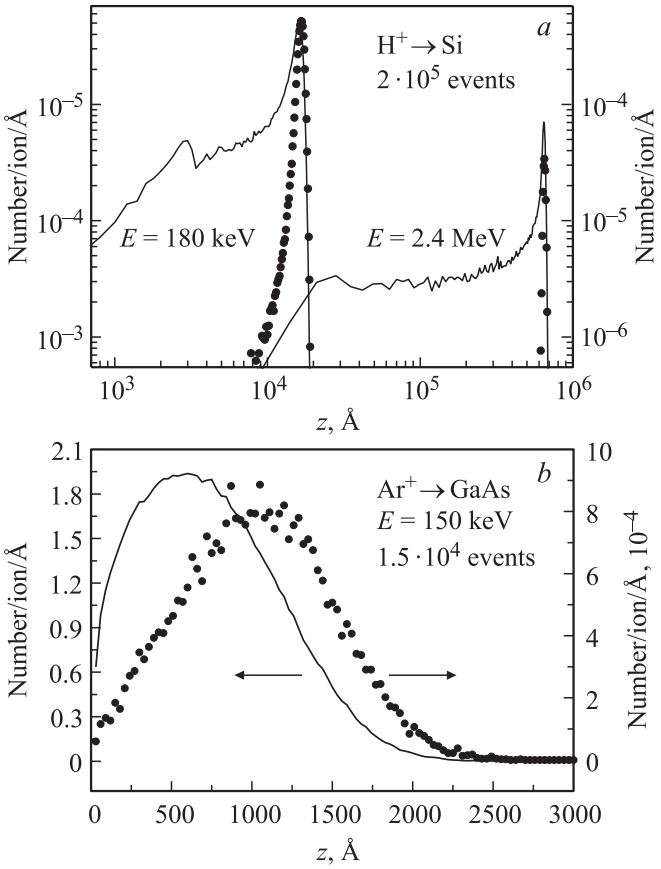

Figure 1. TRIM simulations of the depth distribution of the displaced target atoms (solid lines, left scale) and implanted atoms (dots, right scale) for the implantation of 180 keV, 2.4 MeV H^+ in Si (*a*) and 150 keV Ar^+ in GaAs (*b*).

the projected range R_p (penetration depth) so that the damage density at depths well below R_p can decrease with increasing proton energy, despite the increase of the total energy deposited in elastic collisions (see Fig. 1). This fact must be taken into account when irradiating nanometer thick layers containing, e.g., quantum dots or a quantum well and situated near the sample surface.

The effect of ionization on the defect production in the common semiconductors exists but mostly is a minor one. Anyway, the ionization (formation of electron–hole pairs) alone does not produce RDs in these semiconductors as it is the case in wide-gap insulators. However, the degradation of a MOS device, especially at low irradiation doses, is almost entirely due to the long-lived effects of ionization in the dielectric subelement, i.e. in the gate insulator [14]. In bipolar devices the primary effect of ionizing radiation is gain reduction. This is usually due to an increase in surface recombination near the emitter–base region. Ionization damage also causes leakage current to increase [15].

The sensitivity of the device parameters to irradiation is further determined by material properties, such as the threshold energy for atomic displacement (see above), probability of the annihilation of the self-interstitials and

vacancies, type and level of doping, position of the defect-induced energy levels in the gap. There is a comprehensive literature on the subject of the radiation hardness of semiconductors and semiconductor devices [16].

Summarizing, in order to predict the radiation damage in QSSS, first of all one needs knowledge on the creation, transformation, and annihilation processes of RDs in corresponding bulk materials including alloys. Whereas these processes in Si are well understood, the information concerning Ge is much less detailed. The worst situation is to be stated for the SiGe alloys. To solve the problem of the radiation hardness of a device, one has to establish which layer (or layers) in a concrete, probably very complicated, structure predominantly determines the device parameters degradation. In devices containing low-dimensional active layers, it is important to know which is the volume sampled by the wavefunction of the electrons and holes confined in the layers. Finally, the role of the Fermi level, heterointerfaces and strain in the defect evolution and defect reactions, the mutual influence of the adjacent layers, and the impact of the quantum confinement on the structure and properties of local defects, which are supposed to be already known from the studies of the corresponding bulk semiconductors, have to be elucidated.

On the other hand, what is the useful information we can learn from the irradiation studies?

— Influence of the defects on the electronic properties of QSSS and on the corresponding device parameters;

— elucidation of the electronic structure of QSSS as well as of the carrier transport, relaxation and recombination processes in them using defects as microprobes;

— diffusion processes in QSSS;

— novel technological processes of micro-, nano- and optoelectronics.

The review presents a survey of effects occurring in SiGe quantum wells (QWs), superlattices (SLs) and quantum dots (QDs) upon electron and proton irradiation as well as upon ion implantation. Sec. 2 is dedicated to the important issue of the radiation hardness. It is shown that QD-based devices can withstand much higher radiation fluences than corresponding 2D and bulk structures. The physical mechanisms of this phenomenon are discussed. In Sec. 3, peculiarities of the amorphization of SLs upon ion implantation are considered. Sec. 4 demonstrates examples of the application of particle irradiation to the device technology. At the end, concise conclusions are drawn.

2. Radiation hardness of quantum size heterostructures

2.1. General remarks

The term „radiation hardness“ (the same as „radiation resistance“) describes the ability of a structure's property to withstand the deteriorating action of radiation. The recombination parameters of semiconductors are much more sensitive to RDs than e.g. equilibrium carrier concentration or mobility. RDs with deep levels in the bandgap act as non-radiative recombination centers (lifetime killers) limiting the photoluminescence (PL) and electroluminescence (EL) intensity as well as photosensitivity.

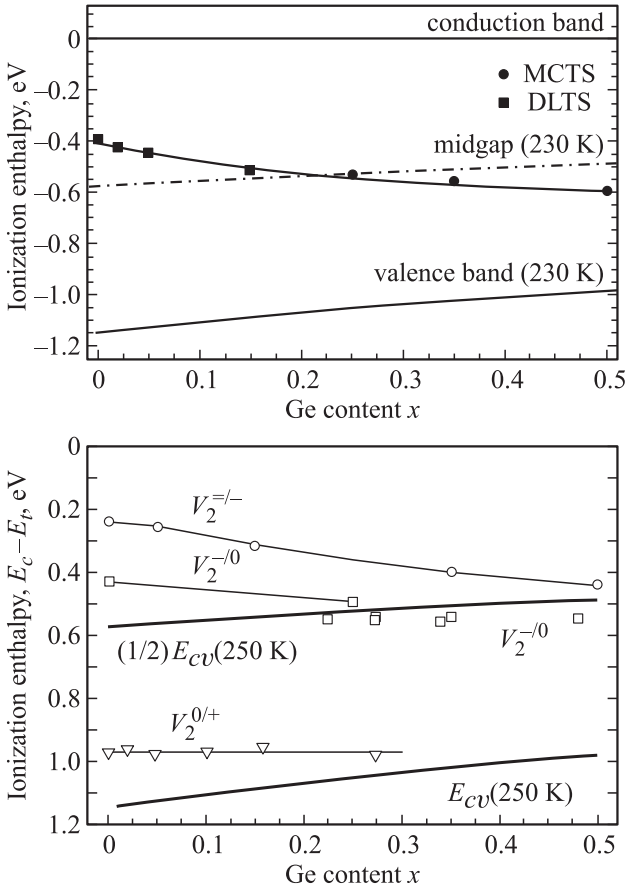

Figure 2. Ionization enthalpies for the E-center defect (left) and of the different divacancy charge states (right) relative to the conduction band E_c of silicon as a function of the Ge content x [40,41].

The increased tolerance of defects is one of the most important promises of the self-assembled QD nanotechnology [17]. The basic argument is that more strongly localized carriers exhibit reduced migration to non-radiative centers. As pointed out in Ref. [18], Turnbull was probably the first to propose, as early as 1950, that small crystals will contain fewer defects [19]. This „self-purification“ was shown [18] to be an intrinsic property of defects in semiconductor nanocrystals, for the formation energies of defects increase as the size of the nanocrystal decreases. This result has been severely criticized [20], nonetheless, we shall see that a very similar effect is obviously observed in irradiated QDs. Importantly, only relatively small dots can be defect-free. So, e.g., when the QDs exceede certain dimensions, dislocations are observed within the dots.

The influence of Ge doping on the accumulation process of radiation defects in silicon irradiated with gamma-rays

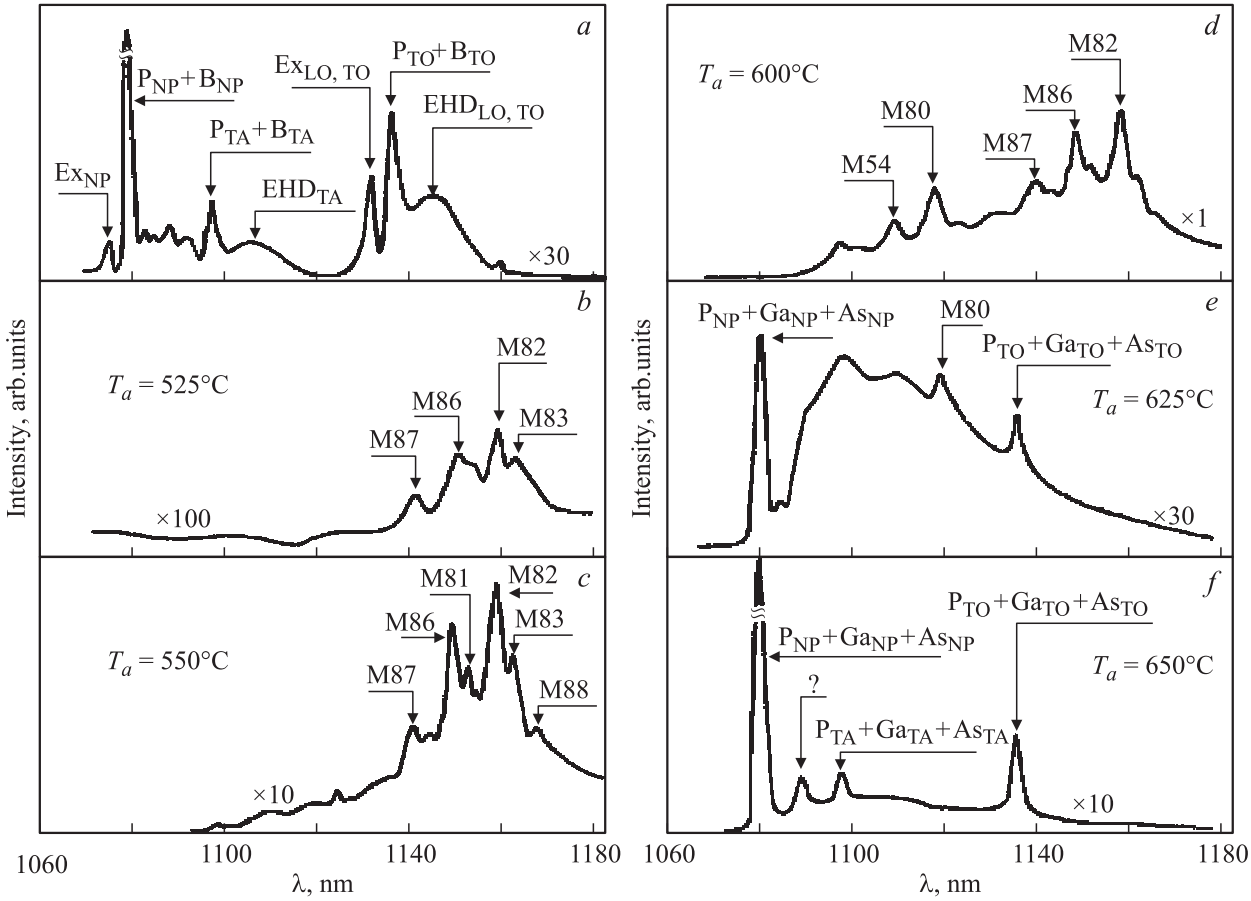

Figure 3. Near-band-edge PL spectra of silicon containing $2 \cdot 10^{20}$ cm^{-3} Ge, as-grown (*a*) and after neutron irradiation and subsequent annealing at the following temperatures, °C: 525 (*b*), 550 (*c*), 600 (*d*), 525+625 (*e*), 550+650 (*f*). Ex means the free exciton. P, Ga, As, and B denote the lines of excitons bound to substitutional phosphorus, gallium, arsenic, and boron atoms, respectively. NP, TA, LO and TO designate non-phonon (NP) transitions and transitions with emission of TA, LO and TO phonons, respectively [44].

and elementary particles has been the subject of numerous investigations (for an early review see, e.g., Ref. [21]). The influence of irradiation on the SiGe-based diodes and MOSFETS is also a subject of intense research (see, e.g., Refs. [22–25]). For quite a long time there had been only one RD containing a Ge atom, namely the Ge–vacancy (Ge–V) pair [26,27], that has been positively identified. However, it anneals well below room temperature. It has been suggested that at irradiation temperatures $T_i \geq 300$ K the Ge atoms act as centers of indirect recombination of Frenkel pair components [28–30]. The further progress has been limited to the detection of the Ge–divacancy pair (Ge–V_2) [31,32].

The influence of the Ge content on the properties of a few point defects known for pure Si has been understood [33–39]. An example is given in Fig. 2. The conclusions drawn from these studies with respect to the defect level position in the gap are as follows [40,41]:

(i) The observed level displacement towards the valence band with increasing Ge is characteristic for (almost) all defect levels.

(ii) Those levels which cross the midgap level change from being an electron trap in the upper half of the band gap to becoming a hole trap in the lower half of the band gap. This is clearly the case for the single-acceptor levels of the *E*-center (a substitutional donor–neighboring vacancy complex).

(iii) None of these levels are pinned to any of the band edges.

The near-band-edge photolumunescence (PL) of irradiated silicon doped with Ge in various concentrations N(Ge) brought about new insights into the problem [42,43]. New PL lines labeled M80–83, 86, 87 have been found at $N(\mathrm{Ge}) \lesssim 10^{19}$ cm^{-3} whose intensity could be correlated with the Ge content. For $N(\mathrm{Ge}) = 2 \cdot 10^{20}$ cm^{-3} and annealing temperatures $525 \geq T_a \geq 600$°C these lines dominate in the PL spectrum [44] (see Fig. 3). It is worth noting that the lines M81–83, 86, 87 emerge, grow and vanish simultaneously. This fact may indicate their common nature.

In proton-irradiated Ge-doped Si layers grown by molecular-beam epitaxy (MBE), we have found that the

PL spectra are different from those measured in Ge-free films and from those previously reported in irradiated bulk Si(Ge). Several new lines have been found in the near-band edge region of the spectrum, whereas many lines typically measured in Ge-free irradiated Si have not been observed [45].

Thus, it has been concluded that at concentrations of the order of $10^{20}\,\mathrm{cm}^{-3}$ and annealing temperatures above 500°C the Ge atoms are the main sinks for the Frenkel pair components.

2.2. Si/Ge superlattices

An enhanced radiation hardness of the PL and EL in thin-layer Si/Ge SLs with periods of 10 or 15 monolayers (Si_6Ge_4 and Si_9Ge_6) as compared to Si/Ge QWs and to bulk Si has been found [46]. The SLs grown by MBE have been subjected to the irradiation with 3–4 MeV electrons. Then PL and EL as well as electrical measurements on corresponding diode structures have been performed (see Fig. 4). The following model has been proposed to explain the observed effect. When Si is irradiated with 3–4 MeV electrons at RT, most of the stable RDs are formed after long-range migration of the primary RDs, i. e. vacancies and self-interstitials, by subsequent interaction and formation of complexes with impurities. At doping levels above $\sim 10^{17}\,\mathrm{cm}^{-3}$ the creation rate of the stable defects becomes independent of the doping level and approaches the primary displacement rate since each primary defect is then captured by an impurity atom [47]. An analogous picture may basically be assumed for bulk Ge. Hence, even for an impurity concentration as high as $10^{19}\,\mathrm{cm}^{-3}$ the average distance between neighbouring impurities is still of the order of 40 Å, and this determines the mean migration length of a primary defect to form a non-radiative center. At the same time, the mean diffusion length to reach an interface in a short-period SL is a few Å only. The interfaces act as sinks and annihilation centers for the mobile primary radiation defects, thus leading to a lower concentration of non-radiative centers than in the bulk material.

Studies of the current–voltage (I–U) characteristics and capacitance–voltage (C–V) profiling of the Si_6Ge_4-SL-based diodes confirmed the enhanced radiation hardness of the latter [48–50] (Fig. 4, *e*).

Hence, the structuring at the nanolevel is indeed crucial for the radiation hardness!

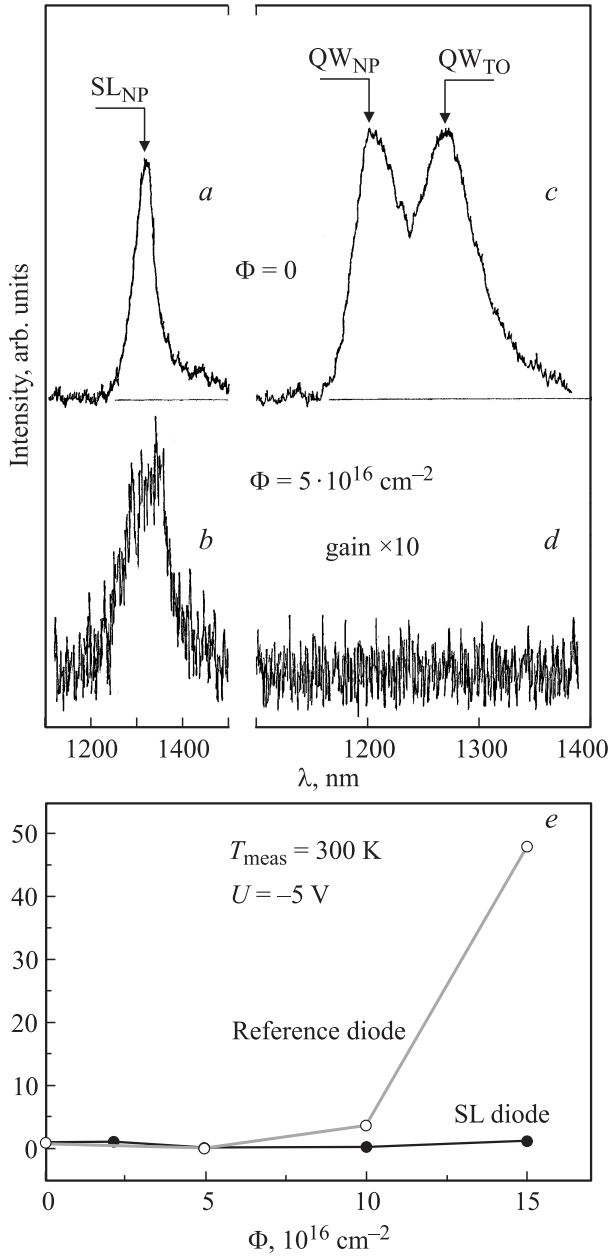

Figure 4. EL spectra of a Si_6Ge_4 SL and a $Ge_2Si_{20}Ge_2$ QW prior to (*a, c*) and after (*b, d*) irradiation with $5 \cdot 10^{16}\,\mathrm{cm}^{-2}$ of 3–4 MeV electrons. $T_{\mathrm{meas}} = 4.2$ K. SL and QW are characteristic luminescence bands of superlattice and quantum well, respectively. NP and TO indices refer to no-phonon transitions and their TO-replica, respectively [75]. (*e*) — reverse current at 300 K vs. 3–4 MeV electron irradiation fluence Φ for a Si_6Ge_4 SL and an industrial diode [49].

2.3. Ge/Si quantum dot heterostructures

The samples containing 10 closely spaced Ge QD layers embedded in a Si matrix have been grown by MBE and irradiated with 2.4 MeV protons [51]. Upon irradiation with this energy the protons penetrate far behind the QD layer (see Fig. 3) and do not exhibit any passivation effect. The irradiation produces an uniform defect concentration up to the several tens of μm depth, reducing the intensities of all spectral components observed prior to the irradiation, but to a different extent. Besides, the irradiation introduces into Si well-known point defects with sharp non-phonon lines (C, G and W) [52,53] and a very broad band, also of defect origin. It is seen in Fig. 5 (right panel) that the PL bands from the 2D wetting layer (WL_{TO} component) and Si matrix (FE_{TO}, BE_{TO}) disappear already for the lowest fluence whereas the PL from the QDs persists. The *X*-ray

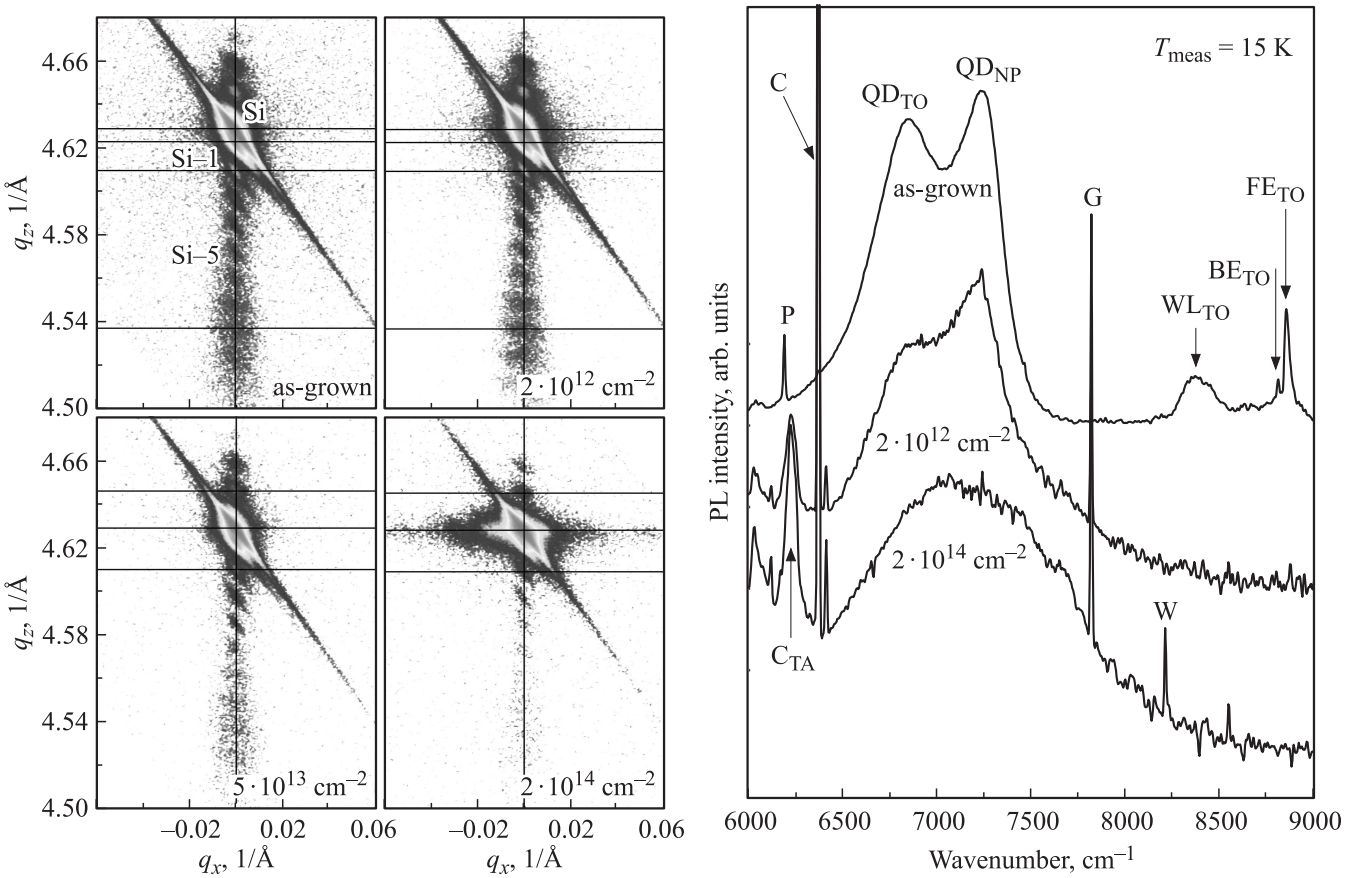

Figure 5. *X*-ray reciprocal space maps (RSM) of the symmetric (004) plane for a Ge/Si QD sample with 10 layers of QDs, as-grown and subjected to 2.4 MeV proton fluences ranging from $2 \cdot 10^{12}$ to $2 \cdot 10^{14}$ cm^{-2} (left), and PL of the same sample prior to and after irradiation with two fluences of 2.4 MeV protons, $2 \cdot 10^{12}$ and $2 \cdot 10^{14}$ cm^{-2} (right). Adopted from [51,76].

reciprocal space maps (RSM, Fig. 5, left panel) exhibit features due to the periodic arrangement of the QD layers up to the highest proton fluence used ($2 \cdot 10^{14}$ cm^{-2}). This behavior clearly proves a higher radiation resistance of the dots as compared to quantum wells (here in the form of a WL) and bulk material.

Beside the obvious role of the confinement of captured charge carriers in the QDs, there might be another physical mechanism of the enhanced radiation hardness of QDs akin to that observed in SLs. Since the primary defects (vacancies and interstitial atoms) are mobile at RT in Si and Ge, it is very likely that they are captured at the QD–matrix interfaces and recombine there (Sec. 2.2 and Ref. [46]). Moreover, the defects raise the free energy of the crystal, so that it is only natural that the QDs expel mobile defect components into the matrix.

When the Ge/Si QD layers are deposited so tightly that they form a superlattice, the radiation hardness of the structure is even higher [54,55]. In spite of the expected high concentration of nonradiative recombination centres caused by the proton-induced damage, the PL emission from the Ge dots has been observed even for the highest irradiation fluence of $2 \cdot 10^{14}$ cm^{-2}.

3. Coherent amorphization in superlattices

Most crystalline materials can be rendered amorphous upon bombardment with energetic ions. However, the critical ion doses needed for the amorphization of different materials vary by orders of magnitude. It is well known that the critical dose of amorphization of silicon is ca. one order of magnitude higher than that of germanium [56,57]. However, the maximum relative damage created in low Ge content films ($x = 10-20\%$) is considerably higher than the values obtained by the interpolation between the results for implanted single-crystalline Si and Ge [57], so that the damage kinetics for $x > 0.4$ is very similar to that of pure Ge [58]. Hence, a selective amorphization of (rather thick) individual layers was expectedly observed upon ion implantation into SiGe/Si (and AlAs/GaAs) multilayer structures [56,59].

A quite opposite result has been obtained by us using the Rutherford backscattering/channeling (RBS) and high-resolution cross-sectional transmission electron microscopy (HR XTEM) on short-period Si_6Ge_4 and Si_9Ge_6 SLs: the Si and Ge layers in the SLs were amorphized simultaneously

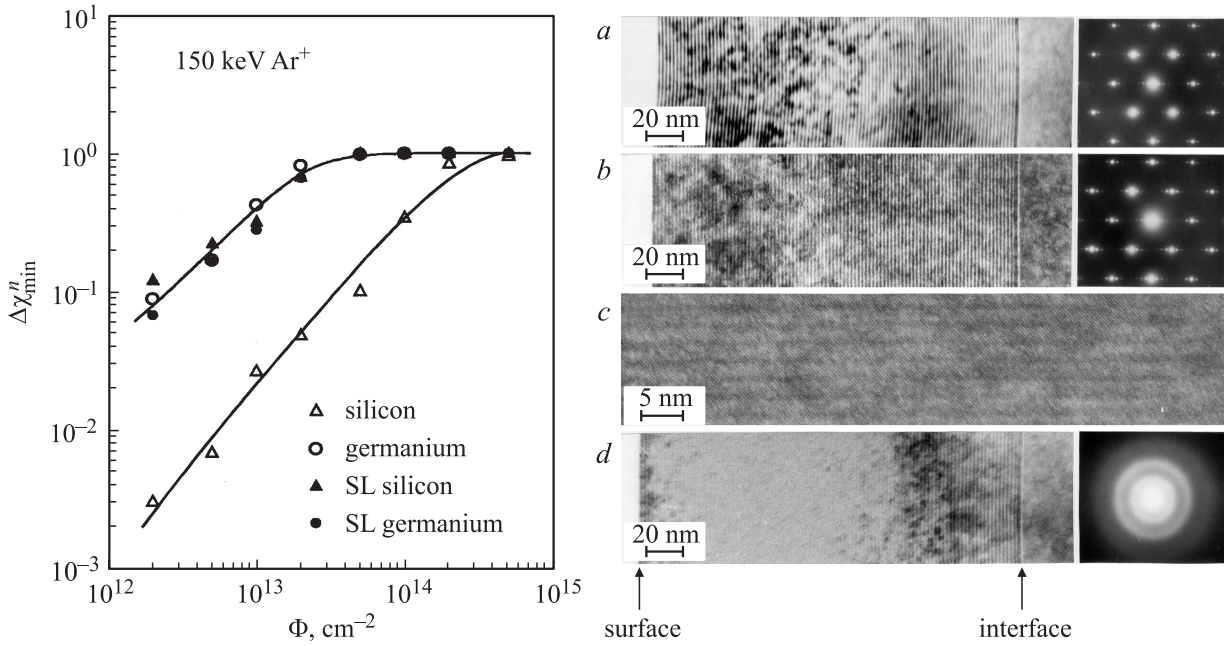

Figure 6. Normalized minimum RBS yield $\Delta\chi^n_{\min}$ (reflecting the relative amount of damage) for the pure crystalline Si and Ge as well as that for the Si and Ge layers in a Si_9Ge_6 SL plotted vs. 150 keV Ar^+ ion fluence Φ [60] (left), and HR XTEM of the same SL at $\Phi = 2 \cdot 10^{13}$ (*a*), $1 \cdot 10^{14}$ (*b, c*), $2 \cdot 10^{14}\,\mathrm{cm}^{-1}$ (*d*) (right). The microdiffraction patterns have been taken from a depth corresponding to the maximum damage [61,62].

at one and the same dose that coincided with the critical dose of bulk germanium [60–62] (see Fig. 6). We assumed that this coherent amorphization of the different layers in a SL can only occur if the SL period (which is only 1.4 or 2.2 nm in the investigated SLs) is shorter than the typical dimension of the individual damage clusters originating from the collision cascades induced by the primary recoil atoms.

As it is impossible to grow structurally perfect Si/Ge SLs with arbitrarily thick layers, AlAs/GaAs SLs with different periods along with $Al_xGa_{1-x}As$ alloys with x ranging from 0 to 1 were implanted to check this idea [63,64]. The difference of the amorphization behavior between GaAs and AlAs is even much bigger that between Si and Ge [65]. AlAs actually cannot be amorphized by implantation at room temperature, so the implantations and RBS measurements were done at cryogenic temperatures without intermediate warming up of the samples. The SL with a period of $(1.4 + 1.4)$ nm behaved like an alloy with $x = 0.5$, whereas the behavior of that with a period of $(10 + 10)$ nm was already quite peculiar. Thus, it is very probable that the above-mentioned coherent amorphization of the Si and Ge layers in short-period Si/Ge SLs is a consequence of the fact that these SLs behave like SiGe alloys with the same integral Ge content. Further, a layer thickness of 10 nm is already „above threshold“: the AlAs/GaAs SL does not behave anymore like an alloy, there is no coherent amorphization of different layers. Finally, for the AlAs/GaAs SL with a period of $(70 + 83)$ nm a selective damage and amorphization behaviour was clearly observed in the RBS spectra [63,64]. As was shown in Ref. [66], the broadening of an initially 0.27 nm wide AlAs/GaAs interface inside the damage cluster of a single ion amounts to ~ 2 nm. Hence, our results point to the intermixing in the collision cascades as one of the reasons of the observed coherent SL amorphization.

However, more work is necessary to definitely answer the question on the role of intermixing in this phenomenon. As a matter of fact, the XTEM images show that a clear contrast of the Si and Ge layers is observed up to amorphization [60–62] (see Fig. 6, *d*). Even after having been amorphized, the SLs are not completely intermixed: a weak contrast is present in the XTEM micrographs, which is caused by different atomic numbers of Si and Ge. Generally, the amorphization occurs when the resultant Gibbs free energy of a crystalline region and of defects accumulated in it exceeds that of the corresponding amorphous region and does not require a total intermixing *per se*.

4. Radiation technology

Radiation treatment can be used to improve the performance of QSSS-based devices or to modify their characteristics in a desired manner. A typical change of the $I-U$ characteristic of a Si_6Ge_4 SL diode as a result of 3–4 MeV electron irradiation measured at $T_{\mathrm{meas}} = 77$ K is shown in Fig. 7 [67]. With increasing fluence Φ, the curve shifts to higher voltages. Moreover, for $\Phi \geq 1.5 \cdot 10^{17}\,\mathrm{cm}^{-2}$ a range of negative differential resistance (NDR, an *S*-shaped characteristic) appears. The origin of the *S*-shaped forward

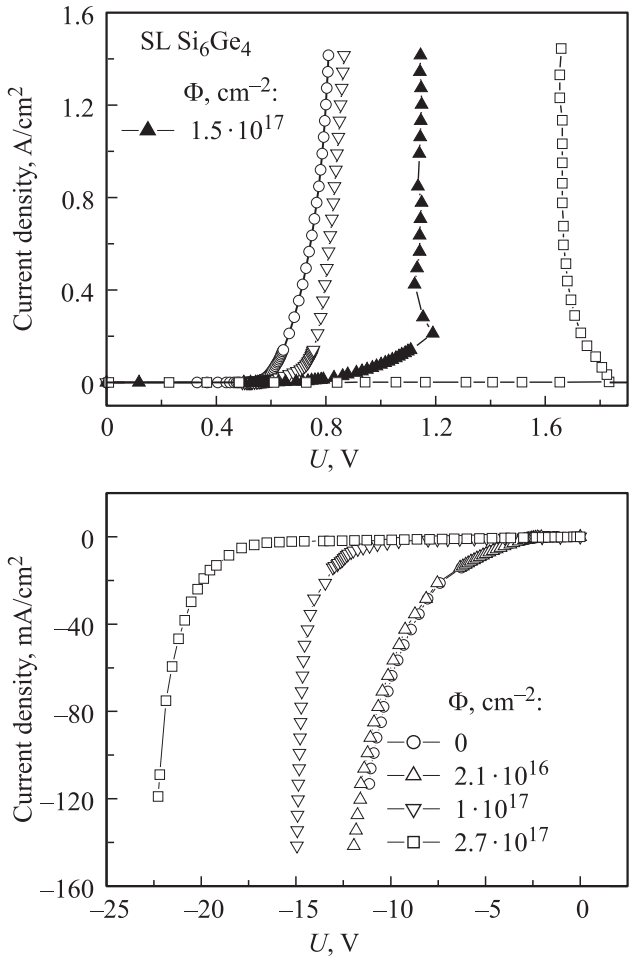

Figure 7. Current–voltage characteristics at 77 K of a Si_6Ge_4 superlattice diode subjected to 3–4 MeV electron irradiation with various doses [67].

$I-U$ characteristic is not yet quite clear and is subject of further investigations. An S-shaped $I-U$ characteristic was reported in long-period GaAs doping SLs and ascribed to avalanche multiplication in the high-field regions of the SL and accumulation of holes in the valence-band maxima [68]. However, the characteristic has not been observed in corresponding short-period SLs, which was ascribed to the fact that in this case tunneling through thin barriers dominated over perpendicular transport. Anyway, a regenerative switching device can be developed using the observed phenomenon.

An interesting application of irradiation in the QSSS technology is the low-energy ion-beam-assisted Ge growth on Si [69–71]. Pulsed ion-beam action results in the increase of Ge nanoislands density and decrease of average island size and size dispersion. The experiments have been combined with molecular dynamics simulations. The effect has been ascribed to the ion-beam-induced formation of surface vacancies and bulk interstitial atoms. The vacancies play the role of effective traps for Ge adatoms, while the interstitials create local stretched regions at the surface. Both factors promote the nucleation of 3D Ge nanoislands.

Ion-induced intermixing is particularly important in the fabrication of integrated nanosize heterostructures (e. g. GRINSCH, graded-index separate confinement heterostructure) [72]. Independently of the amount of intermixing in the collision cascades discussed in Sec. 3, the mixing in Si–Ge heterostructures can be strongly enhanced by post-irradiation heat treatment and occurs due to defect-enhanced diffusion. Our experimental results have clearly shown [73] that the ion implantation causes an irreversible damage of the SiGe SLs. The subsequent annealing leads to a breakdown of the SL structure due to the intermixing of the Si and Ge layers resulting in the transformation of the SL into an alloy. The temperatures involved are much lower than those typical of the interdiffusion in an undamaged SiGe SL. Thus, this technology may be useful in the fabrication of highly integrated SiGe circuits [74].

5. Conclusions

Some recent results on the influence of particle irradiation on SiGe quantum size structures have been discussed. The SLs and, to a much higher extent, QDs exhibit an enhanced radiation hardness, which is especially important in atomic energy and space-born telecommunication applications. The radiation-induced defects not only deteriorate the parameters of the structures and corresponding devices, but they also can be used to obtain devices with new characteristics. So, a negative differential conductivity has been obtained in electron-irradiated Si/Ge SLs. The dependence of the amorphization kinetics of different layers in a SL on their thickness upon ion implantation in Si/Ge SLs reveals an intimate relation to intermixing phenomena in solids.

The work has been supported in part by the project PEst-C/CTM/LA0025/2011 of the FCT of Portugal.

References

[1] E.G. Stassinopoulos, J.P. Raymond. Proc. IEEE, **76**, 1423 (1988).
[2] D. Kanjilal. Curr. Sci., **80**, 1560 (2001).
[3] P.S. Gwozdz, J.S. Koehler. Phys. Rev. B, **6**, 4571 (1972).
[4] J. Bourgoin, M. Lannoo. *Point defects in semiconductors II, Experimental aspects* [Springer Ser. in Sol. St. Sci., v. 35] (Springer, Berlin, Heidelberg, 1983).
[5] F.F. Morehead, B.L. Crowder. Rad. Eff. Def. Solids, **6**, 27 (1970).
[6] J.F. Gibbons. Proc. IEEE, **60**, 1062 (1972).
[7] S. Takeda, J. Yamasaki. Phys. Rev. Lett., **83**, 320 (1999).
[8] J. Yamasaki, S. Takeda, K. Tsuda. Phys. Rev. B, **65**, 115 213 (2002).
[9] H. Bernas. In: *Radiation Effects in Solids*, ed. by K.E. Sickafus et al. (Springer, Dordrecht, 2007) chap. 12, p. 353, and references therein.
[10] P. Sigmund. In: *Sputtering by Particle Bombardment I*, ed. by R. Behrisch (Springer, Berlin, 1981).

[11] J.F. Ziegler, J.P. Biersack, U. Littmark. *The Stopping and Range of Ions in Solids* (Pergamon, N.Y., 1985); http://www.srim.org/
[12] Available from the Radiation Shielding Information Center, Oak Ridge National Laboratory, P.O. Box 2008, Oak Ridge, TN, 37831-6362, USA, pdc@epic.epm.ornl.gov.
[13] P. Hovington. Scanning, **19**, 29 (1997).
[14] *Ionizing Radiation Effects in MOS Devices and Circuits*, ed. by T.P. Ma, P.V. Dressendorfer (John Wiley, N.Y., 1989).
[15] A.H. Johnston. *4th Intern. Workshop on Rad. Eff. in Semicond. Devices for Space Appl.* (Tsukuba, Japan, 2000).
[16] See, e.g.: IEEE Trans. Nucl. Sci.; Proc. Intern. Conf. on Defects in Semicond.
[17] C. Weisbuch, J. Nagle. In: *Science and Engineering of 1D and 0D Semiconductor Systems*, ed. by C.M. Sotomayor-Torres and S.P. Beaumont [NATO ASI Series B124] (Plenum, N.Y., 1990) p. 319.
[18] G.M. Dalpian, J.R. Chelikowsky. Phys. Rev. Lett., **96**, 226 802 (2006).
[19] D. Turnbull. J. Appl. Phys., **21**, 1022 (1950).
[20] M.-H. Du, S.C. Erwin, Al.L. Efros, D.J. Norris. Phys. Rev. Lett., **100**, 179 702 (2008).
[21] N.A. Sobolev. In: *Physics Chemistry and Application of Nanostrucutres* (World Scientific, Singapore, 1997) p. 43.
[22] C. Claeys, E. Simoen. *Radiation effects in advanced semiconductor materials and devices* (Springer Verlag, N.Y., 2002).
[23] H. Ohyama, T. Nagano, K. Takakura, M. Motoki, K. Matsuo, H. Nakamura, M. Sawada, S. Kuboyam, M.B. Gonzalez, E. Simoen, G. Eneman, C. Claeys. Thin. Sol. Films, **518**, 2517 (2010).
[24] H. Ohyama, N. Naka, K. Takakura, I. Tsunoda, M.B. Gonzalez, E. Simoen, C. Claeys. Microelectronic Eng., **88**, 484 (2011).
[25] H. Ohyama, K. Shigaki, K. Hayama, K. Takakura, M. Yoneoka, Y. Takami, J. Vanhellemont, E. Simoen, C. Claeys. Res. Rep. Kumamoto-NCT, **1**, 93 (2009).
[26] G.D. Watkins. IEEE Trans. Nucl. Sci., **NS-16**, 13 (1969).
[27] G.D. Watkins, J.R. Troxell, A.P. Chatterjee. Inst. Phys. Conf. Ser., **46**, 16 (1979).
[28] L.I. Khirunenko, V.I. Shakhovtsov, V.V. Shumov. Fiz. Tekh. Poluprovodn., **32**, 132 (1998) [Semiconductors, **32**, 120 (1998)].
[29] V.G. Golubev, V.V. Emtsev, P.M. Klinger, G.I. Kropotov, Y.V. Shamartsev. Fiz. Tekh. Poluprovodn., **26**, 574 (1992) [Sov. Phys. Semicond., **26**, 328 (1992)].
[30] M.S. Saidov, S.L. Lutpullaev, A. Yusupov, I.G. Atabaev, L.I. Khirunenko, N.A. Matchanov, D. Saidov, M.U. Hajiev. Fiz. Tverd. Tela, **49**, 1582 (2007) [Phys. Solid State, **49**, 1658 (2007)].
[31] L.I. Khirunenko, Yu.V. Pomozov, M.G. Sosnin, M.O. Trypachko, A.V. Duvanskii, N.V. Abrosimov, H. Riemann, S.B. Lastovskii, L.I. Murin, V.P. Markevich, A.R. Peaker. Mater. Sci. Semicond. Processing, **9**, 525 (2006).
[32] L. Khirunenko, Yu. Pomozov, M. Sosnin, N. Abrosimov, W. Schröder. Physica B, **308**–**310**, 550 (2001).
[33] L.I. Khirunenko, Yu.V. Pomozov, M.G. Sosnin, A. Duvanskii, V.J.B. Torres, J. Coutinho, R. Junes, P.R. Briddon, N.V. Abrosimov, H. Riemann. Physica B, **401**–**402**, 200 (2007).
[34] S. Hayama, G. Davies, J. Tan, V.P. Markevich, A.R. Peaker, J. Evans-Freeman, K.D. Vernon-Parry, N.V. Abrosimov. Physica B, **340**–**342**, 823 (2003).
[35] J.P. Leitão, A. Carvalho, J. Coutinho, R.N. Pereira, N.M. Santos, A.O. Ankiewicz, N.A. Sobolev, M. Barroso, J. Lundsgaard Hansen, A. Nylandsted Larsen, P.R. Briddon. Phys. Rev. B, **84**, 165 211 (2011).
[36] A. Mesli, Vl. Kolkovsky, L. Dobaczewski, A. Nylandsted Larsen, N.V. Abrosimov. Nucl. Instrum. Meth. Phys. Res. B, **253**, 154 (2006).
[37] A. Mesli, A. Nylandsted Larsen. J. Phys.: Condens. Matter, **17**, S2171 (2005).
[38] V.P. Markevich, A.R. Peaker, L.I. Murin, N.V. Abrosimov. J. Phys.: Condens. Matter, **15**, S2835 (2003).
[39] A.R. Peaker, V.P. Markevich. In: *Silicon Heterostructure Handbook: Materials, Fabrication, Devices, Circuits and Applications of SiGe and Si Strained-Layer Epitaxy*, ed. by J.D. Cressler (CRC Taylor & Francis, 2006) p. 107.
[40] H. av Skardi, A.B. Hansen, A. Mesli, A.N. Larsen. Nucl. Instrum. Meth. Phys. Res. B, **186**, 195 (2002).
[41] A. Nylandsted Larsen, A. Bro Hansen, A. Mesli. Mater. Sci. Eng. B, **154**–**155**, 85 (2008).
[42] A.V. Voevodova, F.P. Korshunov, N.A. Sobolev, A.A. Stuk. Fiz. Tekh. Polyprovodn., **23**, 45 (1989) [Sov. Phys. Semicond., **23**, 734 (1989)].
[43] A.V. Voevodova, F.P. Korshunov, N.A. Sobolev, A.A. Stuk. In: *Defect Control in Semicond.* (Amsterdam, 1990) v. 1, p. 387.
[44] N.A. Sobolev, M.H. Nazaré. Physica B, **273**–**274**, 271 (1999).
[45] A.O. Ankiewicz, N.A. Sobolev, J.P. Leitão, M.C. Carmo, R.N. Pereira, J. Lundsgaard Hansen, A. Nylandsted Larsen. Nucl. Instrum. Meth. Phys. Res. B, **248**, 127 (2006).
[46] N.A. Sobolev, F.P. Korshunov, R. Sauer, K. Thonke, U. König, H. Presting. J. Cryst. Growth, **167**, 502 (1996).
[47] V.I. Gubskaya, P.V. Kuchinskii, V.M. Lomako. Rad. Eff. Def. Solids, **55**, 35 (1981).
[48] E.S. Basova, S.B. Lastovskii, N.A. Sobolev, F.P. Korshunov, U. König, H. Presting. Intern.: *Topical Problems of Solid-State Electronics and Microelectronics. Proc. 5th All-Russian and Intl. Conf.* (Taganrog, TRTU, 1998) p. 71.
[49] E.S. Basova, S.B. Lastovskii, N.A. Sobolev, F.P. Korshunov, U. König, H. Presting. *8th Intern. Conf. „Radiation Physics of Solids"* (Sevastopol, 1998).
[50] N.A. Sobolev, E.S. Basova, S.B. Lastovskii, F.P. Korshunov, N.A. Poklonskii, A.I. Syaglo, M.H. Nazaré, H. Presting, U. König. *Abstracts 20th Intern. Conf. Defects Semicond.* (Berkeley, USA, 1999) p. 293.
[51] N.A. Sobolev, A. Fonseca, J.P. Leitão, M.C. Carmo, H. Presting, H. Kibbel. Phys. Status Solidi C, **0**, 1267 (2003).
[52] G. Davies. Phys. Rep., **176**, 83 (1989).
[53] R. Sauer. In: *Landolt–Börnstein* (Springer, Berlin, 1989) v. 22b, P. 338.
[54] A. Fonseca, N.A. Sobolev, J.P. Leitão, E. Alves, M.C. Carmo, N.D. Zakharov, P. Werner, A.A. Tonkikh, G.E. Cirlin. J. Luminesc., **121**, 417 (2006).
[55] J.P. Leitão, N.A. Sobolev, M.R. Correira, M.C. Carmo, N. Stepina, A. Yakimov, A. Nikiforov, S. Magalhães, E. Alves. Thin Sol. Films, **517**, 303 (2008).
[56] D.J. Eaglesham, J.M. Poate, D.C. Jacobson, M. Cerullo, L.N. Pfeiffer, K. West. Appl. Phys. Lett., **58**, 523 (1991).

[57] D.Y.C. Lie, A. Vantomme, F. Eisen, T. Vreeland, Jr., M.-A. Nicolet, T.K. Carns, V. Arbet-Engels, K.L. Wang. J. Appl. Phys., **74**, 6039 (1993).
[58] T.E. Haynes, O.W. Holland. Appl. Phys. Lett., **61**, 61 (1992).
[59] M. Vos, C. Wu, I.V. Mitchell, T.E. Jackman, J.-M. Baribeau, J. McCaffrey. Appl. Phys. Lett., **58**, 951 (1991).
[60] N.A. Sobolev, K. Gärtner, U. Kaiser, U. König, H. Presting, B. Weber, E. Wendler, W. Wesch. Mater. Sci. Forum, **248**–**249**, 289 (1997).
[61] N.A. Sobolev, U. Kaiser, I.I. Khodos, H. Presting, U. König. *Mater. Res. Soc. Symp. Proc.* (Wareendale, PA, USA, 1999) v. 540, p. 91.
[62] N.A. Sobolev, U. Kaiser, I.I. Khodos, H. Presting, U. König. Izvestia RAN, Ser. fiz., **63**, 1352 (1999) [Bull. Russian Acad. Sci., Physics Ser., **63**, 1066 (1999)].
[63] N.A. Sobolev, M.C. Carmo, B. Breeger, E. Wendler, W. Wesch, R. Hey, H.T. Grahn. *Intern. Conf. Electronic Mater. and EMRS Spring Meeting* (Strasbourg, 2000).
[64] N.A. Sobolev, M.V. Carmo, B. Breeger, E. Wendler, W. Wesch, R. Hey, H.T. Grahn. *15th Intern. Conf. Ion Beam Analysis, IBA-15* (Cairns, 2001).
[65] B. Breeger, E. Wendler, Ch. Schubert, W. Wesch. Nucl. Instrum. Meth. Phys. Res. B, **148**, 468 (1999).
[66] M. Bode, A. Ourmazd, J. Cunningham, M. Hong. Phys. Rev. Lett., **67**, 843 (1991).
[67] N.A. Sobolev, E.S. Basova, S.B. Lastovskii, F.P. Korshunov, N.A. Poklonskii, A.I. Syaglo, M.H. Nazaré, H. Presting, U. König. *Abstracts 2nd All-Russian Conf.* „*Silicon-2000*“(Moscow, 2000) p. 107.
[68] E.F. Schubert, J.E. Cunningham, W.T. Tsang. Appl. Phys. Lett., **51**, 817 (1987).
[69] A.V. Dvurechenskii, J.V. Smagina, V.A. Zinovyev, S.A. Teys, A.K. Gutakovskii. Int. J. Nanosci., **3**, 19 (2004).
[70] N.P. Stepina, A.V. Dvurechenskii, V.A. Ambrister, J.V. Smagina, V.A. Volodin, A.V. Nenashev, J.P. Leitão, M.C. Carmo, N.A. Sobolev. Thin Sol. Films, **517**, 309 (2008).
[71] Zh.V. Smagina, P.L. Novikov, V.A. Zinovyev, V.A. Armbrister, S.A. Teys, A.V. Dvurechenskii. J. Cryst. Growth, **323**, 244 (2011).
[72] For a review of QW intermixing, see, e. g., IEEE J. Select. Topics Quant. Electron., **4** (4) (1998), and references therein.
[73] N.A. Sobolev, J. Gerster, G. Mauckner, M. Wolpert, W. Limmer, K. Thonke, R. Sauer, H. Presting, U. König. Nucl. Instrum. Meth. Phys. Res. B, **136**–**138**, 1057 (1998).
[74] D.J. Paul. Semicond. Sci. Technol., **19**, R75 (2004).
[75] N.A. Sobolev, H. Presting, unpublished.
[76] M.A.L. Fonseca. PhD thesis (Universidate de Aveiro, 2007).

Редактор Л.В. Шаронова